A MODEL FOR PREDICTING THE STIFFNESS OF BEAM TO CONCRETE FILLED COLUMN AND MINOR AXIS JOINTS UNDER STATIC MONOTONIC LOADING

Luís Costa Neves
Assistant Professor
Department of Civil Engineering
University of Coimbra, Portugal
E-mail: luis@dec.uc.pt

Luís Simões da Silva
Professor
Department of Civil Engineering
University of Coimbra, Portugal
E-mail: luisss@dec.uc.pt

Pedro C. G. S. Vellasco
Associate Professor
Department of Structural Engineering
University of the State of Rio de Janeiro, Brasil
E-mail: vellasco@.uerj.br

ABSTRACT

In this paper, a model for predicting the initial stiffness of the column web or face in bending is described. It is based on an equivalent strip, spanning in one direction, reflecting the actual structural behaviour. The experimental evidence from monotonic minor axis and I beam to concrete-filled RHS column joints tests is briefly presented. Finally, a systematic procedure for assessing the rotational behaviour of the column web in minor axis joints, in line with the basic principles of the component method, with restrained and unrestrained flanges, and of the column face in RHS concrete filled columns is proposed, and some indications about the accuracy of the model are given.

1 INTRODUCTION

Eurocode 3 (EC3) part 1.8 [1], proposes a general methodology to predict the behaviour of the joints, the so-called "component method", that is based on a mechanical model where each spring characterizes a source of deformability – the component. Providing that any component has a previously established structural response in terms of force-displacement behaviour, it is then possible to establish the relevant rotational properties of any joint configuration.

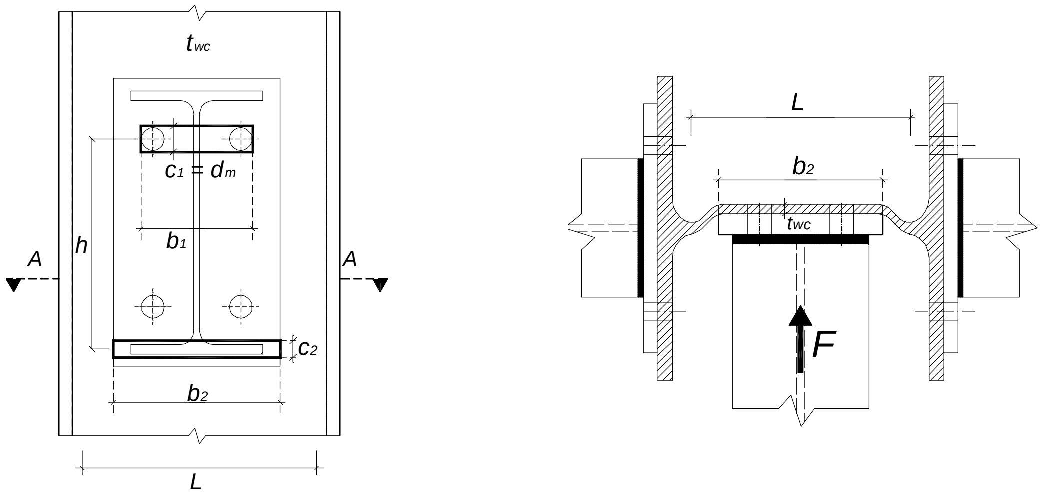

a) Joint geometry and dimensions b) Column web deformed in bending

Fig. 1: Minor axis beam-to-column joints

In the particular case of minor axis joints (Fig. 1a), EC3 [1] limits the application of the component method to internal nodes with symmetrical loading. This is a particular case where no bending moment is transmitted to the column through its web, that therefore does not contribute to the joint deformation, similarly to a beam splice response. However, if the moments from both sides of the column are unequal, the column web is deformed transversally in bending as represented in Fig. 1b.

Another joint geometry where a plate in transverse bending may have a dominant role is illustrated in Fig. 2. This is the case of an I beam connected to the face of a RHS column, also similar to the column web behaviour in a minor axis joint.

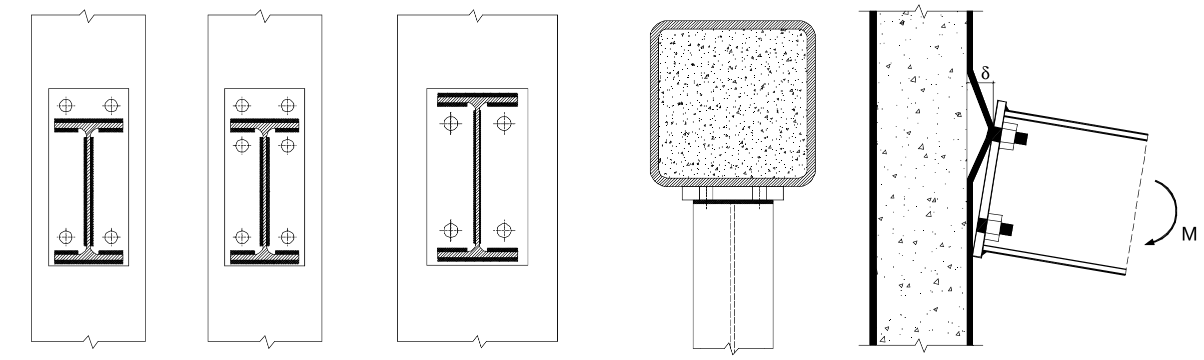

a) Config. (1) b) Config. (2) c) Config. (3) d) Column face deformed in bending

Fig. 2: I-beam to concrete-filled RHS column joints

This typical component behaviour is illustrated in Fig. 3a. An initial linear elastic stiffness $S_{j,ini}$ (for which a model is presented in this paper) is followed by a stiffness reduction associated to progressive yielding. The loading level corresponding to this stiffness decrease is usually approximated by a plastic moment M_{pl}, commonly evaluated using yield line theory [4]. A frequently used model is the Gomes model, based in log spiral fan yielding patterns [2]. Finally, it is noted that a significant post-limit stiffness, related to plate membrane stiffness S_{jm}, is usually present.

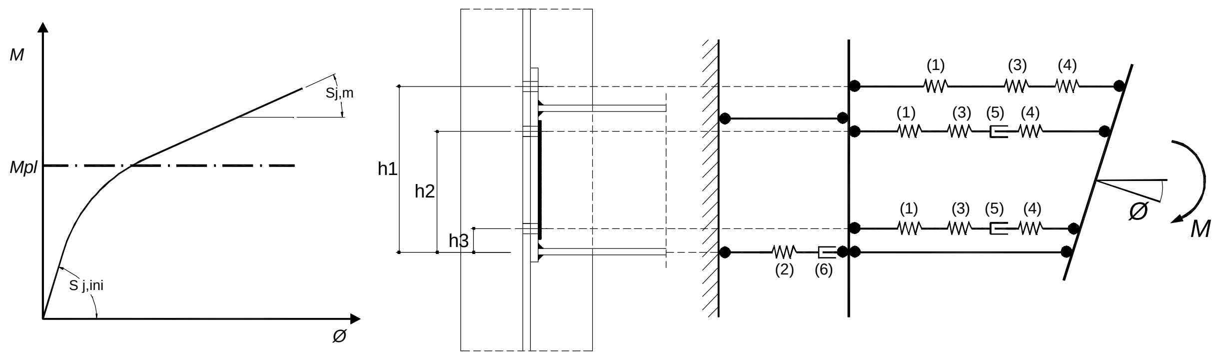

a) Typical behaviour b) Mechanical model

Fig. 3: Component behaviour and Eurocode 3 mechanical model for deriving the joint $M-f$ curve from the $F-d$ behaviour of the individual components – extension to a minor axis joint.

The extension of the EC3 to these geometries requires the implementation of a model to characterise the column web or face bent transversally (new component), and the inclusion of this deformation source in the mechanical model. In Fig. 3b this adaptation is illustrated for a minor axis extended end plate joint configuration (Fig. 1), where the components are: column web loaded transversally in tension (1); and in compression (2); end plate in bending (3); bolts in tension (4); beam web in tension (5) and beam web and flange in compression (6).

2 EXPERIMENTAL EVIDENCE

An experimental testing program was carried out at the Civil Engineering Department of the University of Coimbra comprising both configurations described above. Details of the testing program and instrumentation may be found in [6] and [5] respectively for minor axis or for RHS joints. The adopted instrumentation enabled the derivation of the stress distribution, deformation pattern of the component and the measurement of the forces at each bolt row.

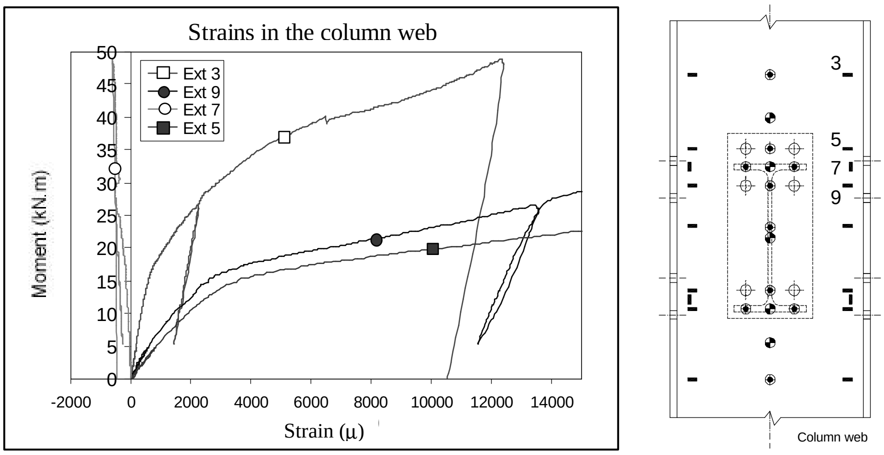

Fig. 4: Steel a minor axis joint: experimental strains in the column web (two bolt rows in tension).

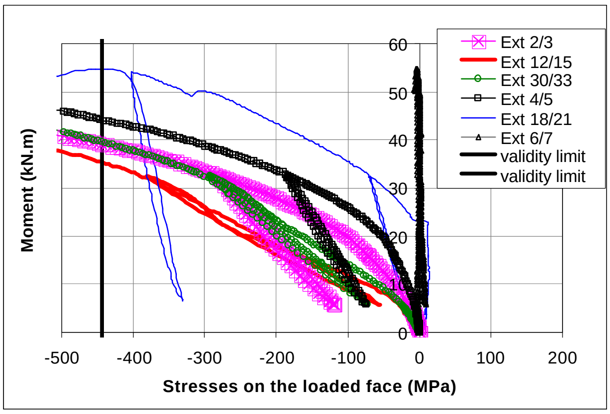

a) Horizontal average stresses on the column face

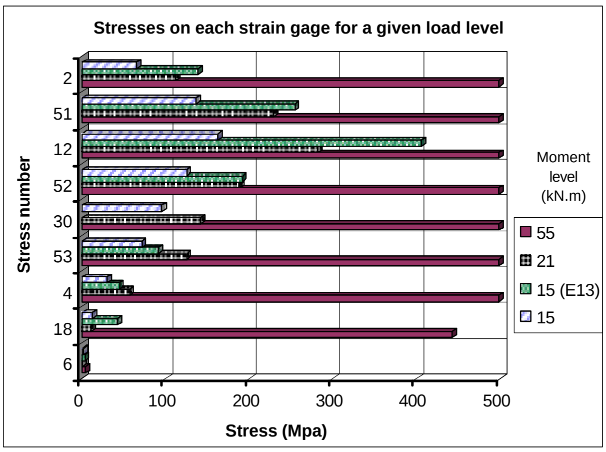

b) Vertical distribution of the horizontal stresses

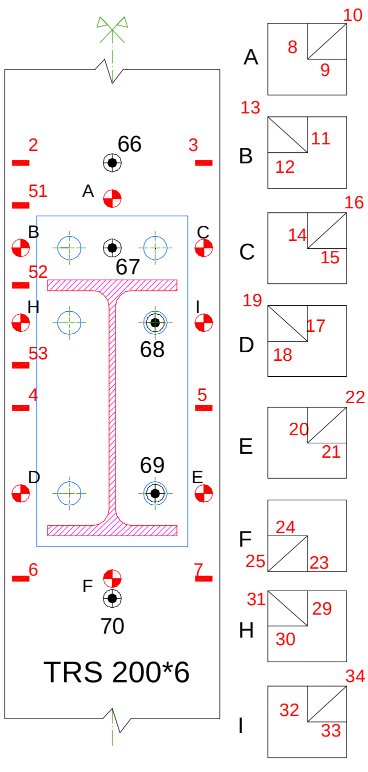

c) Stress identification

Fig. 5: Stress distribution at the column loaded face – RHS column.

This component behaves, in the elastic range, essentially in the direction between the flanges or the lateral faces. As an illustration for a minor axis joint, Fig. 4 shows test strains located at points designated as 3 to 9. It may be concluded from the moment-strain curves that the higher stresses are in line with the uppermost bolt row, and they decrease with the vertical distance to this line. In addition, the stress measured in the perpendicular direction (no. 7) was quite small, showing the behaviour as a strip spanning in one direction.

The illustration of these facts for a RHS column is shown in Fig. 5. The average stresses at each level, in terms of moment-stress curves are plotted in Fig. 5a, taking into account the joint symmetry. It is interesting to observe that there are virtually no stresses close to the compressive area (at the bottom), since the infilling concrete effectively supports the face. The maximum value corresponds to the line of the upper stud row (12/15), where first yield occurs. It is also possible to observe a decrease in stress intensity in points located further away from this load line. The bars in Fig. 5b are plotted for two moment levels smaller than the plastic capacity (about 32 *kN.m*) i.e.: 15 and 21 *kN.m*. The stress distribution at a 15 *kN.m* moment level for E13 test (without the second stud row), is also plotted. Finally, the stress distribution near the connection failure depicting a wide spread yielding pattern is also shown. It may be concluded that until this generalised yielding is attained it is possible to assume an elastic distribution of stresses and, consequently, elastic forces in the stud rows. In addition, principal directions are very close to the vertical and to the horizontal axis, with low stresses in the vertical direction, confirming the one-dimensional strip behaviour [5].

2 MODEL FOR THE INITIAL STIFFNESS

2.1 Strip model for the translational stiffness

Previous studies, namely [2], [4], have established the dimensional parameters governing the component behaviour: the width *b* and the height *c* (mean diameter of the bolt shank d_m in the tensile area) of the compressive and tension force transmission areas supposed as rigid; the column web (or face) thickness t_{wc} and its dimension *L*. In this paper an adequate value for *L* is proposed based on a extensive numerical study. From these dimensions, some non-dimensional parameters can be established: $m = L/t_{wc}$, $\beta = b/L$ and $\alpha = c/L$.

The model assumes the previously described unidirectional component behaviour and that the flanges or the lateral faces of the column restrain the rotation of the web / loaded face. As a result, a one-way spanning strip is defined, with a length *L* and a width l_{eff} , fixed at the two supports - Fig. 6. These support conditions are met for concrete-filled RHS but, for minor axis joints, the presence of major axis beams is required, as in Fig. 1.

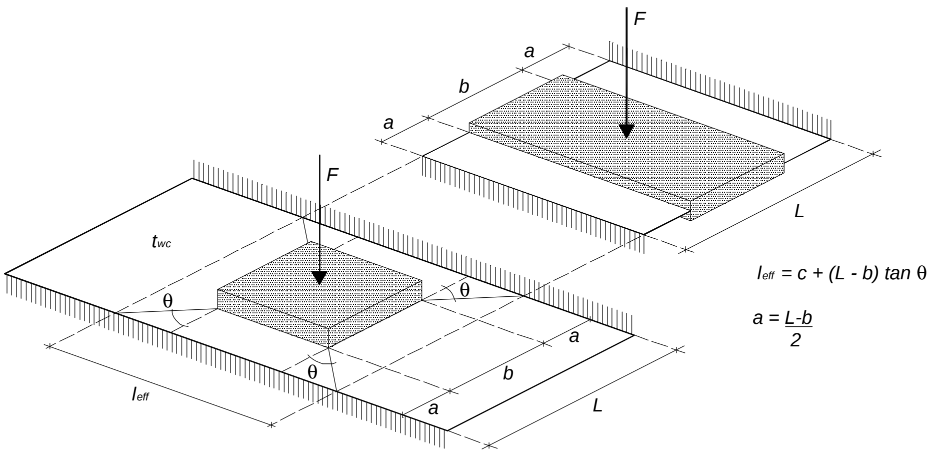

Fig. 6: Component loaded by a rigid area $b \times c$, and equivalent strip of width l_{eff} .

The component translational elastic stiffness is:

$$S_i = \frac{Et_{wc}^3}{L^2} 16 \frac{a + (1-b)\tan q}{(1-b)^3 + \frac{10,4(k_1 - k_2 b)}{m^2}} \tag{1}$$

where E Young’s modulus;

t_{wc} Thickness of the column web/face;

L Representative dimension of the column web/face (see 2.2);

a , b and m are defined in paragraph 1;

$k_1 = 1{,}5$ and $k_2 = 1{,}6$ are coefficients obtained from numerical calibration;

q Angle that defines l_{eff} : $q = 35 - 10b$ if $b < 0.7$ and $q = 49 - 30b$ if $b = 0.7$

The application of this model is limited to $10 \le m \le 50$; $0{,}08 \le b \le 0{,}75$; $0{,}05 \le a \le 0{,}2$. A bending behaviour is assumed, accounting for shear deformations, excluding cases where punching shear dominates, as it is the case for larger values of b . In practice this is not so limitative for minor axis joints, since in these cases, it is possible to weld the beam flanges to the column flanges, obtaining a fully resistant joint [4].

2.2 Representative dimension of the column web/face, *L*

The representative dimension of the component *L* may, for RHS columns, be considered as the distance between the mid-thickness of the lateral faces (Fig. 7a) [4], and for minor axis joints, as the straight part of the web plus a part of the filled radius, *a*: $L = d + 2a$ (Fig. 7b).

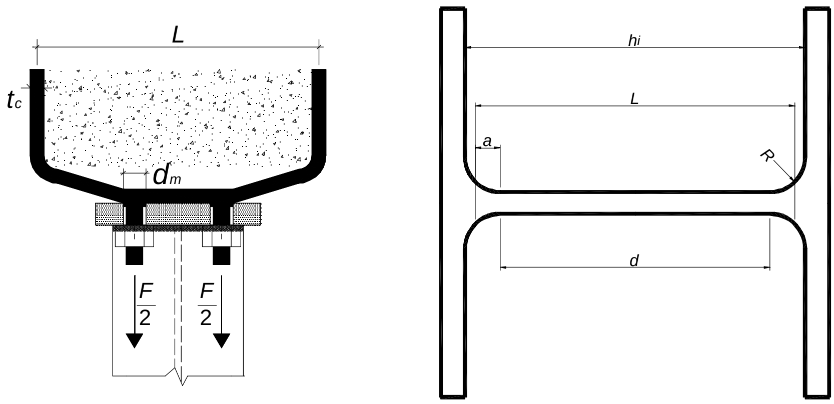

a) *L* in RHS columns b) *L* in minor axis joints

Fig. 7: Definition of the representative dimension of the component, *L*.

There are several proposals for *a*, like the EC3 value of $a = 0{,}2r$, established for plastic analysis, that leads to $L = d + 0{,}4r$. In the elastic range, however, *a* should be calibrated, since it has a great influence over the stiffness. In fact, as an example, for a particular geometry tested in [4], the translational stiffness at the tensile and compressive areas is respectively 47% and 81% higher when *a* varies from $a = 0.6r$ to $a = 0.2r$, corresponding to a variation in *L* of only 8.5%. A finite element calibration, considering solid elements with the fillet radius and equivalent clamped strips of span *L*, led to the conclusion that an adequate value is $a = 0.5r$, leading to the proposed value of $L = d + r$.

2.3 Minor axis joints with unrestrained column flanges

If no major axis beams are present, the stiffness is reduced, as the column flanges rotate. A similar model for the translational stiffness as in paragraph 2.1 may be deducted- Fig. 8.

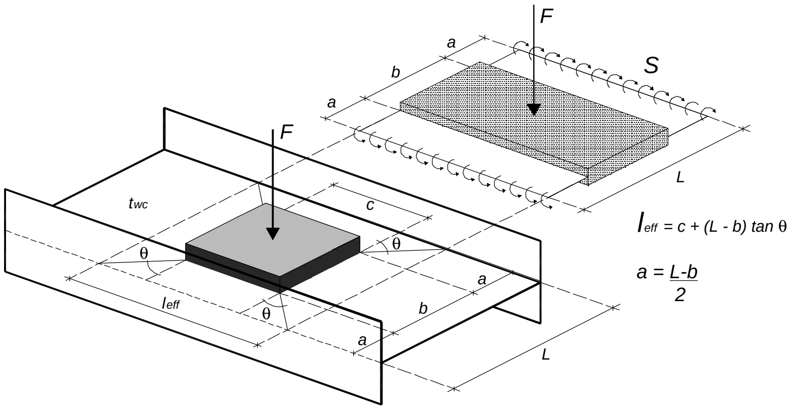

Fig. 8: – Component loaded by a rigid area – unrestrained column flanges.

The corresponding elastic stiffness neglecting the shear contribution, assuming a rigid loading area and equal effective torsional stiffness of both flanges, $S_{f1} = S_{f2} = S_f$ is:

$$S_i = \frac{4Et_{wc}^3}{L^2} \frac{a + (1-b)\tan q + 6S_f \dfrac{1-b}{Et_{wc}^3}}{(1-b)^3\left[1 + \dfrac{3S_f}{2} \dfrac{1-b}{Et_{wc}^3\left(a + (1-b)\tan q\right)}\right]} \tag{2}$$

The calibration of the parameters involved in equation (2), specially the stiffness of the web continuous bending support at the extremes S_f (i.e. the effective torsional stiffness of the flanges) is not an easy task. In fact, the effective restriction of the flanges to the web rotation depends on many factors: effective length of the flanges mobilised in torsion; distance between the applied compression and tension forces; dimensions of the loading areas; failure mode; relative stiffness of the web and flanges, among others. As a consequence, a reduction factor to be applied to the stiffness of restrained flanges, obtained from equation (1), is proposed to derive the stiffness in the case or unrestrained flanges. It is based on the analysis of data from numerical simulations and 41 tests performed at the University of Liège [2], [3], after verifying that this stiffness reduction depends mostly on m and b - Fig. 9. Equation 3 gives the elastic stiffness for this situation, noting that no reduction is needed if $m/b \geq 70$.

$$S_{i,\,freeflanges} = \frac{(m/b)^{1,25}}{230} S_{i,\,fixedflanges} \leq S_{i,\,fixedflanges} \tag{3}$$

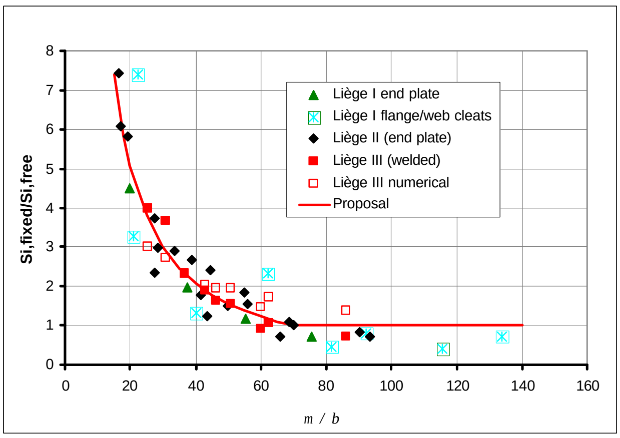

Fig. 9: – Stiffness reduction as a function of m/b .

2.4 Joint Rotational Stiffness

The joint rotational stiffness may be derived from the model in Fig. 3b, taking for the corresponding stiffness coefficients (1) and (2), the results from equation (1), with adequate values for q and L. In particular, Fig. 10 illustrates the application of the model to derive the rotational stiffness of the column web or face in case of two bolt rows in tension.

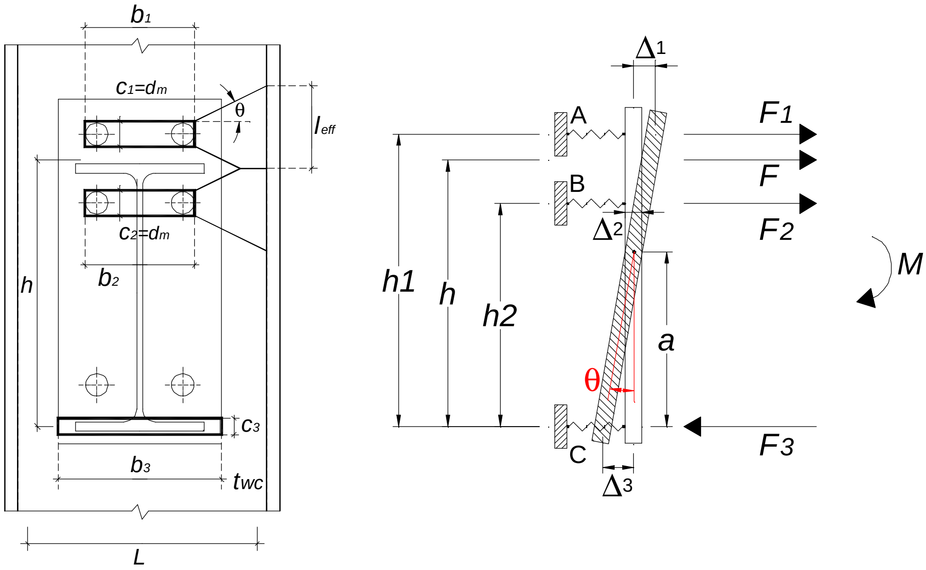

Fig. 10: Model for deriving the $M-f$ curves from the $F-d$ curves of each bolt row.

The analysis of the model assuming the usual situation of $S_1 = S_2 = S$ leads to an expression for the joint rotational elastic stiffness $S_{j,ini}$, where the notation is shown in Fig. 10:

$$S_{j,ini} = Sh_1\left(h_1 - \frac{h_1 + h_2}{\frac{S_3}{S}+2}\right) + Sh_2\left(h_2 - \frac{h_1 + h_2}{\frac{S_3}{S}+2}\right) \qquad (4)$$

In the case of one bolt row in tension, the missing bolt row i is taken with $S_i = 0$.

2.5 Examples

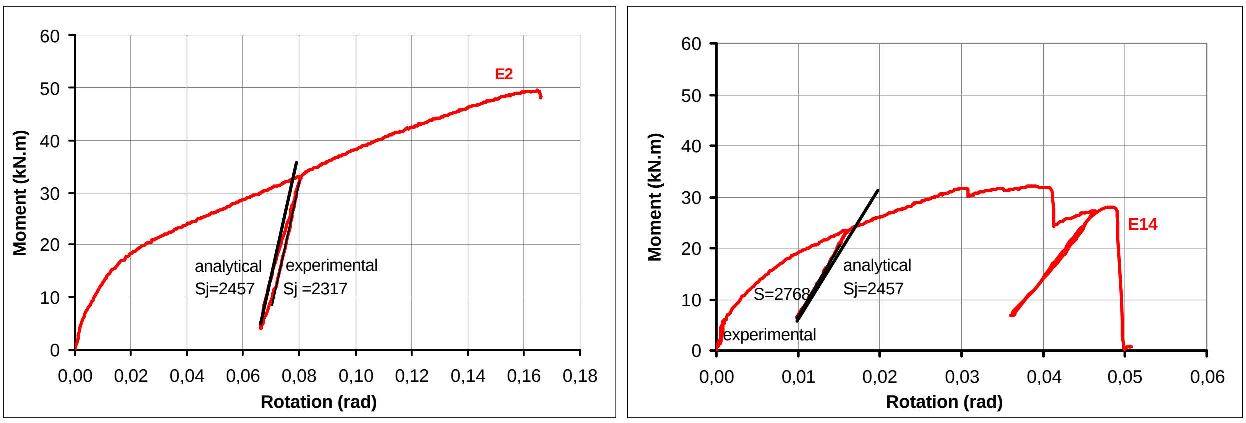

a) Application to a minor axis joint (E2 in [4])   b) Application to a RHS joint (E14 in [4])

Fig. 11: Application of the model to experimental results, example of minor axis and RHS joints [4].

Fig. 11 illustrates the application to the case of a minor axis joint (a) and of a RHS column joint (b). Globally, the application of the above models to available experimental results ($M-f$ curves and $F-d$ curves when available) of minor axis joints and of concrete-filled RHS columns from sources [4] and [7] has shown a good accuracy of the model. Details of this comparison may be found in [4].

An important remark is related to the elastic stiffness on the experimental curves that should be measured at the unloading path of the $F-d$ or $M-f$ curves (Fig. 11).

3 SUMMARY

A model to derive the translational initial stiffness of the component web or RHS column face was presented. Some qualitative experimental results were presented and discussed, aiming at supporting the model assumptions. A proposal for the representative length of the component *L*, was also presented.

An extension of the EC3 component model to minor axis joints and concrete-filled RHS in terms of rotational stiffness was developed. The proposed model could be applied to joints with one or two bolt rows in tension and was based on a linear distribution of forces from the tensile bolt rows, observed experimentally, in the elastic range.

REFERENCES

[1] CEN - Eurocode Nº 3 - Design of Steel Structures. Part 1.8: design of Joints - European Standard EN 1993-1-1, Commission of the European Communities, Brussels, 2003.

[2] Gomes, F.C.T., Jaspart, J.P., Maquoi, R., "Moment capacity of beam-to-column minor-axis joints", *Proceedings of the IABSE International Colloquium on Semi-Rigid Structural Connections*, Istanbul, Turkey, IABSE, 1996, pp 319-326.

[3] Maquoi, R., Jaspart, J.P., Guisse, S., Lognard, B., Taquet, F., Etude expérimentale et théorique du comportement des noeuds poutre-colonne d'axe faible, Sixième rapport semestriel, Recherche COST C1 Région Wallonne – Université de Liège, 1995.

[4] Neves, L.F.C., Monotonic and Cyclic Behaviour of Minor-axis and Hollow Section Joints in Steel and Composite Structures, *Doctoral Thesis*, University of Coimbra, 2004.

[5] Neves, L.F.C, Silva, L.A.P.S., Vellasco, P.C.G., Experimental behaviour of end plate I-beam to concrete filled rectangular hollow section column joints, *International Journal of Applied Mechanics and Engineering*, vol. **9**(1), 63-80, 2004.

[6] Neves, L.F.C., Silva, L.A.P.S., Vellasco, P.C.G., Experimental Behaviour of End Plate Minor Axis Steel and Composite Joints under Static Monotonic Loading. *Proceedings of the Third European Conference on Steel Structures (Eurosteel III)*, Coimbra, 19-20 September 2002, vol. II: 1101-1110. Coimbra: Lamas, A. & Silva, L. edts.

[7] Vandegans, D., Liaison entre poutres métalliques et colonnes en profils creux remplis de béton, basée sur la technique du goujonnage, *CRIF MT 193*, Brussels, 1995.

KEYWORDS

Minor axis joints, Joints in RHS columns, translational stiffness, joint stiffness, elastic stiffness, strip model, component method, experimental analysis of minor axis joints.